Schizophrenia Bulletin vol. 48 no. 3 pp. 712–720, 2022
https://doi.org/10.1093/schbul/sbab149
Advance Access publication January 6, 2022

White Matter Metabolite Relaxation and Diffusion Abnormalities in First-Episode Psychosis: A Longitudinal Study

Xi Chen[1,2,3], Xiaoying Fan[1,2], Xiaopeng Song[1,2,3], Margaret Gardner[1,2], Fei Du[1,2,3], and Dost Öngür[1,3,*]

[1]Psychotic Disorders Division, McLean Hospital, Belmont, MA, USA; [2]McLean Imaging Center, McLean Hospital, Belmont, MA, USA; [3]Department of Psychiatry, Harvard Medical School, Boston, MA, USA

*To whom correspondence should be addressed; Psychotic Disorders Division, McLean Hospital, AB3 South 342. 115 Mill St., Belmont, MA 02478, USA; tel: 617-855-2779, fax: 617-855-2895, e-mail: dongur@partners.org

Microstructural abnormalities in the white matter (WM) are implicated in the pathophysiology of psychosis. In vivo magnetic resonance spectroscopy (MRS) can probe the brain's intracellular microenvironment through the measurement of transverse relaxation and diffusion of neurometabolites and possibly provide cell-specific information. In our previous studies, we observed differential metabolite signal abnormalities in first episode and chronic stages of psychosis. In the present work, longitudinal data were presented for the first time on white matter cell-type specific abnormalities using a combination of diffusion tensor spectroscopy (DTS), T2 MRS, and diffusion tensor imaging (DTI) from a group of 25 first episode psychosis patients and nine matched controls scanned at baseline and one and two years of follow-up. We observed significantly reduced choline ADC in the year 1 of follow-up (0.194 μm²/ms) compared to baseline (0.229 μm²/ms), followed by a significant increase in NAA ADC in the year 2 follow-up (0.258 μm²/ms) from baseline (0.222 μm²/ms) and year 1 follow-up (0.217 μm²/ms). In contrast, NAA T2 relaxation, reflecting a related but different aspect of microenvironment from diffusion, was reduced at year 1 follow-up (257 ms) compared to baseline (278 ms). These abnormalities were observed in the absence of any abnormalities in water relaxation and diffusion at any timepoint. These findings indicate that abnormalities are seen in in glial-enriched (choline) signals in early stages of psychosis, followed by the subsequent emergence of neuronal-enriched (NAA) diffusion abnormalities, all in the absence of nonspecific water signal abnormalities.

Key words: psychosis/NAA/choline/T2 relaxation/diffusion/longitudinal

Introduction

Brain regions are connected through white matter (WM) tracts, and multiple lines of evidence suggest that microstructural abnormalities in the white matter are important in the pathophysiology of psychosis.[1–3] WM abnormalities are related to psychotic symptoms and poor cognitive functioning.[4–6] There is a lengthy and productive history of studying post-mortem tissue to probe WM abnormalities in psychiatry.[7–9] With DTI, structural connectivity abnormalities such as decreased fractional anisotropy (FA) and increased diffusivity has been reported in patients with schizophrenia[10,11] and bipolar disorder.[12] On the other hand, the specific nature and pathophysiology of white matter abnormalities remain unclear, as DTI measures are relatively nonspecific insofar as they do not clearly differentiate between axon- and myelin-specific abnormalities.[13] Mechanistically, differentiation of neuronal and glial signals may elucidate specific pathophysiological processes in psychosis.

Magnetic resonance spectroscopy (MRS) can provide an additional window to the brain's cellular microenvironment through the measurement of transverse (T2) relaxation time and diffusion of neurometabolites. Unlike water, metabolites are enriched within cells and their relaxation/diffusion properties depend mostly on intracellular parameters. Furthermore, some metabolites have a preferential cellular compartmentalization.[14] NAA is dominantly intra-axonal in WM and could provide a specific marker for the neuronal compartment of WM,[15] whereas choline compounds are found in both neurons and glia but enriched in glial cells[16, 17] and thus their diffusion mostly reflects glial microstructure and potentially informs about structural changes between group.[18] Compared to diffusion, which reflects the mean

square displacement traveled by a molecule in unit time, T2 relaxation is determined by spin–spin interactions between the index molecule and its immediate neighbors, e.g., macromolecules. T2 relaxation time and diffusion measures reflect related but distinct aspects of the cellular microenvironment.[19] We have reported reductions in T2 relaxation time of the major MRS visible intracellular metabolites in the gray/white matter of psychosis,[19, 20] indicating that T2 relaxation time could be cell-specific probes to explore neuronal and/or glial abnormalities.

Previously our group has performed a series of studies, using DTS and T2 relaxation time of brain metabolites to study microstructure and macromolecule abnormalities in different brain cell types of psychosis patients.[19, 21–24] We observed elevated NAA ADC, which implied neuron axonal abnormalities in chronic schizophrenia (SZ) patients.[21] In patients with bipolar disorder (BD), the same technique revealed a trend of increased NAA diffusion compared to controls but not reach significance.[22] In a recent study on first-episode psychosis (FEP), we observed significant elevations of both Cr and Cho diffusion in patients with SZ, and elevations of Cho diffusion in patients with BD but no difference in NAA diffusion in either patient group compared to controls.[23] This pattern of results indicated that the aberrant signal may arise preferentially in glia and not neurons in the first episode whereas abnormalities are seen in neuronal signals in chronic illness.

Compared to diffusion, water and NAA T2 relaxation times can provide information on white matter macromolecule structure including myelin and intra-axonal milieu, respectively. In a previous study, we observed an increased water T2 relaxation time as well as a reduced NAA T2 relaxation time in chronic SZ compared to controls.[19] More recently, we further observed that NAA T2 relaxation time is significantly reduced in the chronic psychosis compared to first episode (FE) subjects, suggesting that apparent NAA concentration reductions reported in psychotic disorders may indeed reflect shortened T2 relaxation times and not lower NAA tissue concentration.[24]

These cross-sectional studies have provided information on various aspects of WM pathology at different stages of illness. Regarding the NAA concentration in SZ and psychosis, there was a thorough review recently.[25] Short[26] and long[27, 28] terms longitudinal studies on NAA have been performed in SZ with different outcomes. Decreased Cho in ACC were also observed in longitudinal studies on SZ.[29–31] However, there is no longitudinal study beginning at the early stages of SZ and following patients over time on white matter abnormalities in neuron and glial cells specifically. In the current study, we followed 25 first episode SZ patients as well as nine controls over two years with measurements of metabolite and water diffusion and T2 relaxation to demonstrate active changes in the white matter in the same individuals. This information could bridge the gap of our understanding of disease evolution.

Methods

Participants

Participants experiencing a first episode of psychosis (n = 25) were recruited through the McLean Hospital OnTrack first episode psychosis clinic as part of an ongoing research study. Baseline data from 12 of these participants were included in a recent study.[23] McLean OnTrack is an outpatient program that admits adults ages 18–30 who have experienced new onset of psychosis, with or without mood symptoms, within the past 12 months. 9 age and sex-matched healthy participants were also recruited from the community. Diagnosis was determined by trained staff using the SCID-IV diagnostic interview in conjunction with all available collateral information from medical records, treatment providers, and family members. About 9 of the patients had a schizophrenia-spectrum disorder while 16 had bipolar disorder with psychotic features. All procedures were approved by the Mass General Brigham IRB and all participants provided written informed consent.

Protocols

Clinical assessment and MRI scans were performed at baseline, year 1 and 2 follow-up for the patient group. All 25 subjects returned for the year 1 follow-up and 14 subjects returned for the 2nd year. MRI scans were performed at baseline and year 2 follow-up for the control group with all nine subjects. Clinical and functional measures took approximately 40–60 min to administer. Total MRI experiment time was approximately 70 min.

Clinical assessment

Clinical and community functioning were assessed using the Positive and Negative Syndrome Scale (PANSS), the Young Mania Rating Scale (YMRS), the Montgomery-Asberg Depression Rating Scale (MADRS), and the Multnomah Community Ability Scale (MCAS). The MCAS measures functioning in multiple domains including social interest/effectiveness, independence in daily living, and instrumental role functioning. The North American Adult Reading Test (NAART) was used as a measure of premorbid intelligence quotient (IQ). Information regarding current psychiatric medication use was collected by patient report, and chlorpromazine (CPZ) equivalents were calculated according to the recommendations of Baldessarani et al[32]

MRI

T2 relaxation time and DTS measurements were conducted on a 4 T Varian full body MR scanner (Unity/Inova; Varian NMR Instruments, CA, USA), using a 16-rung, single-tuned, volumetric birdcage coil. Global shimming was preformed followed by anatomy images

acquisition. The details have been described previously (see Supplementary Materials of Du et al[21]). A 1 × 3 × 3 cm^3 single MRS voxel was then placed on in the corona radiata, centered at the level of the genu of the corpus callosum but lateral to it (i.e., does not include any callosal fibers). Its position was anchored by adjacent gray matter in anterior and lateral directions, ensuring that it was placed in comparable location across scans. The tissue segmentation was performed on the T1 images in SPM12. The MRS voxel tissue percentages were calculated using AFNI and the voxel was consistently positioned in WM mostly (88 ± 4% of WM percentage). Localized shimming was performed to ensure water linewidths < 15 Hz.

Metabolite T2 spectra were obtained using a PRESS sequence modified with four varying TEs (30, 90, 120, and 200 ms) and TR = 3000 ms; 48 repetitions for metabolite and 8 repetitions for water T2 relaxation time measurements. A modified PRESS sequence with diffusion gradients was used for DTS measurements. Bipolar diffusion gradients with six directions—(1,1,0) (1,0,1) (0,1,1) (−1,1,0) (−1,0,1) (0, −1,1)—and one control (0,0,0) were applied. The applied b value was 1412 s/mm^2, routinely calibrated using a phantom with water ADC assumed to be 2.1×10^{-3} mm^2/s at room temperature. In these measurements, repetition time/echo time = 3000/135 ms, diffusion time = 60 ms, repetitions = 96 and 4 for metabolites and water diffusion measurements, respectively. In the PRESS sequences of both T2 relaxation time and DTS measurements, a 3 ms sinc pulse with a bandwidth of 2000 Hz was used for excitation; two 6 ms Varian optc4 (Optimized Control Pulse for 4 zero sinc pulse) pulses with a bandwidth of 1050 Hz were used for refocusing. The center of the RF pulses was set to 2.6 ppm. For the excitation pulse, the NAA, Cho, and Cr chemical shift displacements were −5.1%, 5.1%, and 3.4%, respectively. For the refocusing pulses, the NAA, Cho, and Cr chemical shift displacements were −9.7%, 9.7%, and 6.5%, respectively. The excitation pulse was used for the localization of the superior–inferior direction; the two refocusing pulses were used for the localizations of the anterior–posterior and left-right directions. The displaced voxels of NAA and Cho were also presented in figure 1. The water suppression in both measurements was achieved by VAPOR.[33]

DTI was obtained in a Siemens 3 T Trio scanner (Siemens Tim-Trio, Erlangen, Germany). The averaged time between DTI and DTS scans for all subjects were 42 ± 43 days. The DTI data were acquired by axial, single-shot spin echo EPI sequence (TR = 6230 ms; TE = 84 ms; FA = 90°; FOV = 1540 × 1540 mm^2; matrix = 1120 × 1120; slice thickness = 3 mm; slice interval = 3 mm; consecutive scanning of 45 slices). One control image without diffusion weighting and six images with noncolinear diffusion directions at b = 1000 s/mm^2 were acquired.

Processing

The MRS averages were saved individually for all spectra and phase and frequency corrections were applied using FID-A.[34] An amplitude threshold of "mean peak intensity – 2*standard deviation" was applied for each DW spectrum to remove bad averages as suggested in Genovese et al.[35] An exponential weighting of 1 Hz was applied to smooth the spectra. Quantifications of metabolite concentrations were performed with LCModel with eddy current correction using water as reference. The water spectra were also quantified using LCModel.

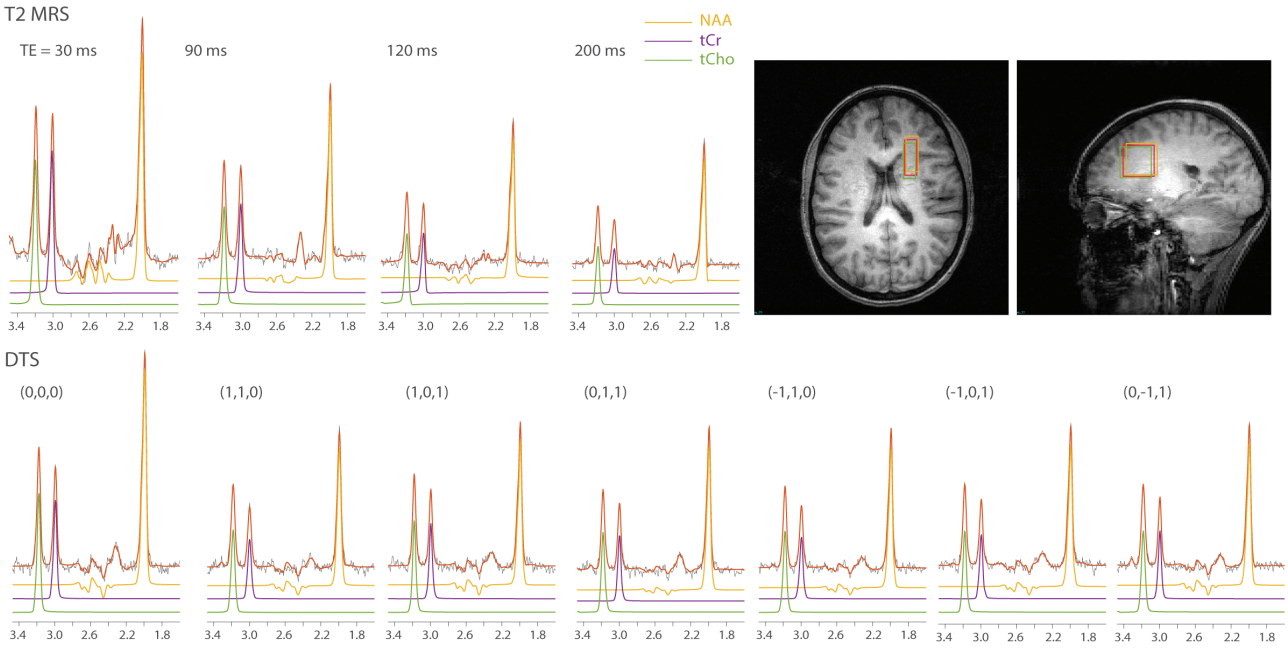

Fig. 1. Representative spectra of T2-MRS and DTS with LC Model fittings, and the voxel position.

The T2 relaxation times of NAA, Cr, Cho, and water were fitted with mono-exponential decay using Matlab. The ADCs of NAA, Cr, and Cho were also calculated in Matlab. The big MRS voxel in DTS studies always average out the anisotropy information of the individual MRI voxels as well as fibers in different directions, i.e., the macroscopic curvature effects.[36, 37] Therefore, FA and the axial/radial diffusivities were not calculated from the big MRS voxel. DTI data were processed and FA and ADC were calculated using FSL.[38] A group-level analysis of the DTI maps was performed in FSL with family wise error (FWE) calculated using the nonparametric permutation test with 5000 permutations. The MRS voxel acquired at 4 T was transformed into standard space and then to the native space of 3 T FA and ADC maps to extract values in the same region. The MRI voxel-wise FA and ADC statistics analyses were performed on the region of the MRS voxel.

Statistics

All statistical analyses were performed using IBM SPSS Statistics Version 25. Linear mixed model analysis was performed on each measure including patient data from the 3 time points to evaluate longitudinal change in the presence of fewer participants in the year 2 follow-up. The scan time point was used as the fixed effect and the repeated effect. The same analyses were performed on the healthy control data from the two time points to test for any scanner drift. T-tests were performed to compare the difference between the patient and control groups at each time point. As the measure of different time points could be highly dependent on one another, we performed the false discovery rate (FDR) test[39] for the multiple comparisons between the patient and control groups in different time points. The FDR threshold was set to 0.05. A Pearson's *R* test was performed to compare the patient group's metabolite ADCs and T2 relaxation times at each time point and between different time points. Pearson's *R* test was also performed to compare the clinical measures (CPZ equivalents, YMRS, MADRS, MCAS, and PANSS) and MRI measures (metabolite T2 relaxation times and ADCs).

Results

Demographic and clinical data for healthy controls and FEP patients are shown in table 1. Representative spectra of T2-MRS and DTS with LCModel fittings, and the voxel position are shown in figure 1. Two subjects' Cr and Cho T2 relaxation times, one at baseline and another at year 1 follow-up, were excluded from the analysis because of poor T2 fitting quality (adjusted $R^2 < 0.8$).

DTS and T2 relaxation times

According to Lin et al,[40] the MRS spectral qualities were reported in supplementary table S1. T2 relaxation time and ADC time courses of NAA, Cr, and Cho of both patient and control groups are shown in figure 2. The scan time factor was significant in the linear mixed model analysis of NAA ADC in FEP patients ($P = .001$) and there was a trend toward significance in Cho ADC ($P = .08$). NAA ADC was significantly higher in year 2 follow-up (0.258 μm²/ms) when compared with year 1 follow-up (0.217 μm²/ms, $P = .001$) and baseline (0.222 μm²/ms, $P = .008$). Cho ADC was significantly lower in year 1 follow-up (0.194 μm²/ms) when compared with baseline (0.229 μm²/ms, $P = .04$). Cr ADC had no significant difference in year 1 and 2 follow-up when compared with baseline. There was no significant finding in any measure of the control group between its two time points (baseline and year 2 follow-up). Figure 4 summarized the contrast between the trajectories of NAA and Cho ADCs. The values of the patient group normalized to healthy controls at the same time point, specifically: baseline and

Table 1. Demographic and Clinical Data

	Healthy Controls	FEP Patients		
	Base ($n = 9$)	Base ($n = 25$)	1st year ($n = 25$)	2nd year ($n = 14$)
Age	23.0 ± 2.9	22.4 ± 2.6		
(range)	(18–27)	(18–27)		
Sex (Female %)	33%	24%		
Education (years)	5.7 ± 1.3	4.9 ± 1.4		
PANSS				
Positive		11.9 ± 6.1	10.5 ± 6.3	10.4 ± 4.8
Negative		12.6 ± 5.4	10.3 ± 3.8	9.6 ± 4.1
General		25.6 ± 6.3	22.5 ± 5.8	22.1 ± 7.9
MADRS		9.4 ± 9.5	6.0 ± 6.9	4.6 ± 6.0
MCAS		45.6 ± 6.6	50.1 ± 5.6	49.1 ± 6.7
YMRS		4.28 ± 4.75	5.14 ± 9.14	4.29 ± 6.27
CPZ equivalent		166.2 ± 155.8	158.2 ± 169.6	140.4 ± 208.3

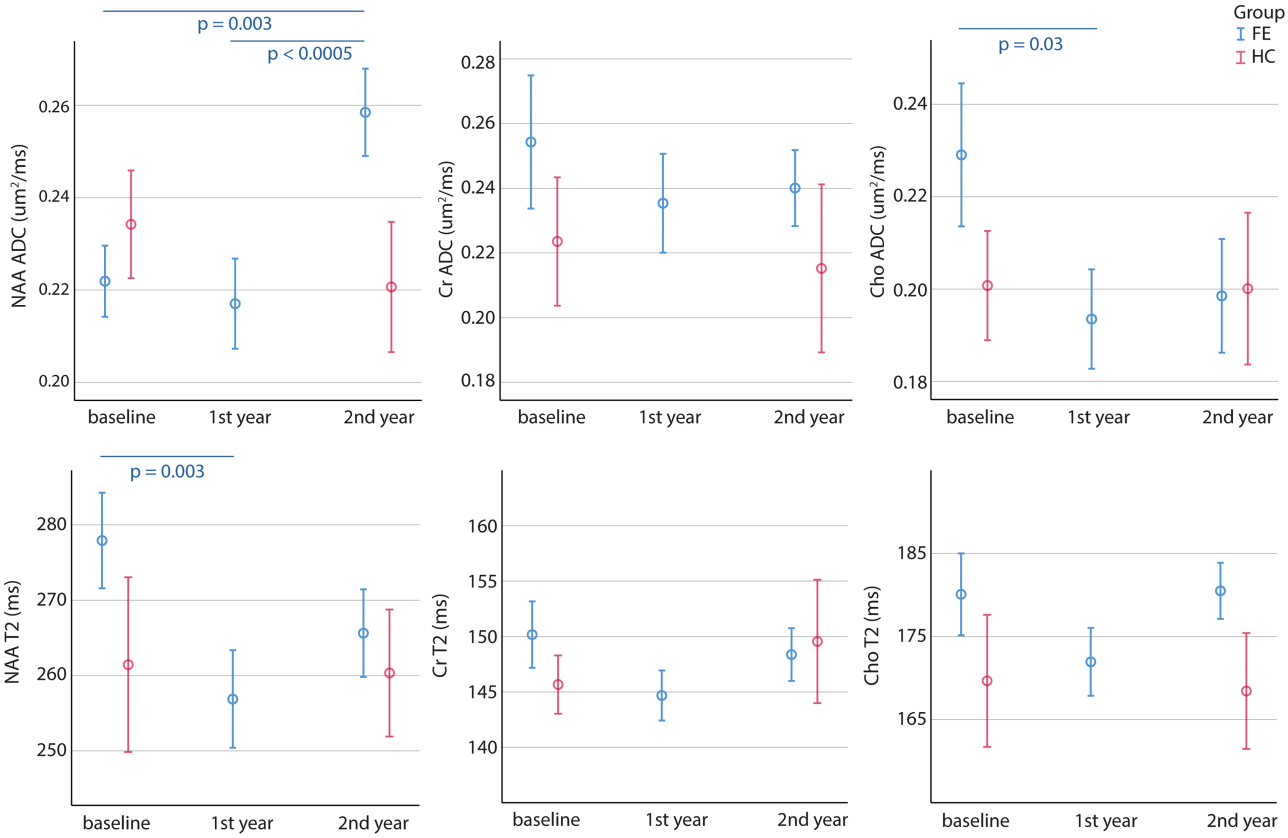

Fig. 2. T2 relaxation time and ADC time courses of NAA, Cr, and Cho of both patient and control groups. The significant *P*-values between different time points are from the Estimates of Fixed Effects of linear mixed model. The error bars represent standard errors.

year 2 of patient group measurements were normalized to the baseline and year 2 of control group, respectively; year 1 of patient group measurements were normalized to the average of the baseline and year 2 of control group.

The scan time factor was significant in the linear mixed model analysis of NAA T2 relaxation time in FEP patients (P = .01), with significant reduction from baseline (278 ms) to year 1 follow-up (257 ms, P = .003) and a trend toward significance between baseline and year 2 follow-up (265 ms, P = .06). There were no significant findings for scan time factor in Cho T2 relaxation time and Cr T2 relaxation time.

When comparing the patient and control groups, only NAA ADC at year 2 follow-up reached a significant difference between the two groups (P = .018, FDR = 0.036). At that timepoint, NAA ADC was elevated not only compared to earlier patient measures but also compared to healthy participants.

Water T2 relaxation time, FA, and ADC

The time courses of T2 relaxation time obtained from water T2 spectra, and the averaged FA and ADC extracted from the MRS voxel on the DTI maps of both patient and control groups are shown in figure 3. Neither the linear mixed model nor *t*-tests between patient and control groups showed any significant differences in any of these analyses.

There was no significant correlation observed between metabolite ADCs and T2 relaxation time at each time point and between different time points. Nor was there any significant correlation between the clinical and MRI measures. No correction for multiple comparison was applied for this exploratory analysis. Despite such a liberal threshold, we did not observe any significant correlations, suggesting that none exist.

Discussion

The present study examined the evolution of abnormalities in various WM signals following a first episode of psychosis. Using advanced MRS methods at 4 Tesla, we collected data on the diffusion and T2 relaxation properties of NAA, Cr, and Cho as well as water. Since NAA is almost exclusively localized to neurons whereas Cho is found in both glial cells and neurons but enriched in glial cells, this design provides an opportunity to examine cell-type-specific abnormalities in psychotic disorders. At baseline, we did not observe any difference between the patient and control groups in any diffusion or T2 measure in our current sample size. At year 1 follow-up, there was a significant reduction in NAA T2 relaxation

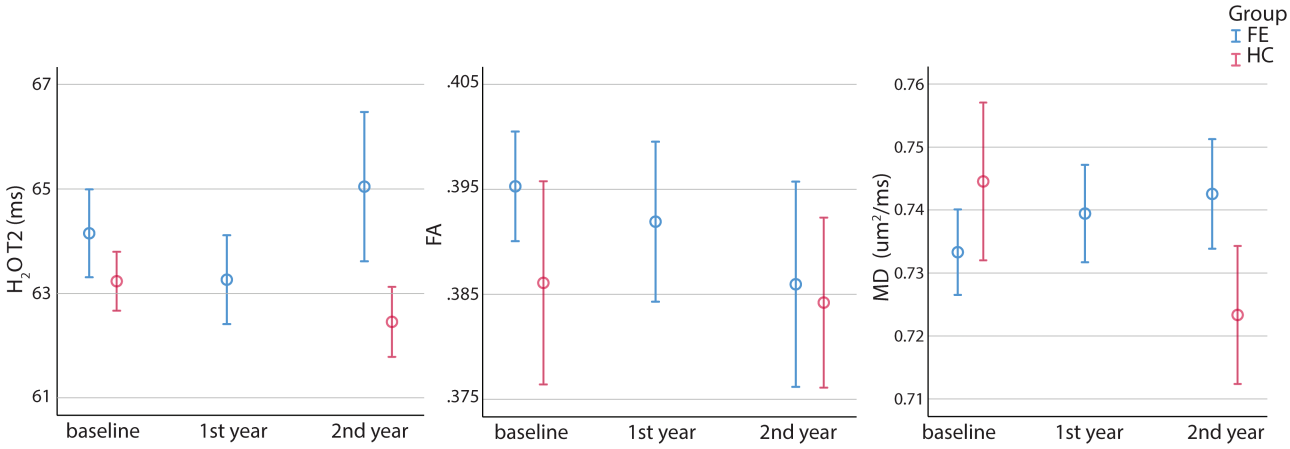

Fig. 3. The time courses of T2 relaxation time obtained from water T2 spectra, and the averaged FA and ADC extracted from the MRS voxel on the DTI maps of both patient and control groups. The error bars represent standard errors.

time, consistent with our most recent reports of reduced NAA T2 relaxation time in chronic psychotic disorders.[24] We also observed an elevation of Cho ADC at year 1 follow-up. At year 2 follow-up, a pronounced elevation emerged in NAA ADC in the FEP group both compared to baseline patient measures and to control measures at follow-up. All of these abnormalities were observed in the absence of any water T2 relaxation time or diffusion abnormalities in FEP patients at any timepoint. The contrast between the trajectories of NAA ADC and Cho ADC is summarized in figure 4.

Early elevations in Cho ADC in the absence of abnormal NAA ADC signal suggest that glial abnormalities may be present in early stages of psychotic disorders. The absence of significant findings in NAA ADC and FA in FEP compared to control suggests that significant abnormalities of axon and myelination morphology are not evident in the very early phase of psychosis, consistent with our recent study.[23] The glia-specific abnormality early in illness could be reflective of neuroinflammation. Studies using a variety of techniques or biomarkers, including cytokines[41] and free water imaging via DTI[42] have reported suggestive evidence of neuroinflammation in early psychosis.

As the disease progressed in follow-up, the Cho ADC signal returned to normal levels in psychosis patients while NAA ADC started to increase. This finding was also in line with our previous findings of abnormal NAA ADC increase in chronic SZ[21] and the trend in BD.[22] Despite the small sample size, we looked into the subgroup plots of longitudinal metabolite ADCs of SZ and BD (supplementary figure S1). The BD group shows less increase in NAA ADC compared to SZ in the follow-up, which is consistent with our previous differential findings in chronic SZ[21] and BD.[22] We interpret our findings as suggesting an active glial process in early psychosis, with subsequent neurodegeneration into chronic illness. The present work further confirms that active neuroprogression in the first episode of illness has not yet

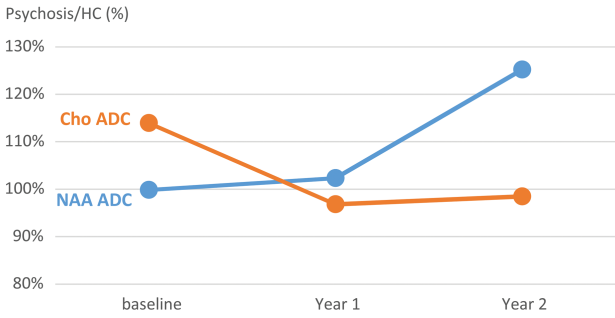

Fig. 4. Psychosis to HC ratios of NAA and Cho ADCs.

resulted in major alterations of axon geometry or myelination, but with time WM abnormalities become more pronounced, particularly in patients with SZ, with subsequent reduction in active glial involvement. Using free water imaging based on DTI,[43] Pasternak et al also reported chronic subjects showed a limited extent of abnormal increase in the volume of the extracellular space, suggesting a less extensive neuroinflammatory response relative to patients at the onset of SZ.[44]

T2 relaxation results from interaction of metabolite molecules with other molecules in the microenvironment and may provide additional insights because it is determined by molecule–microenvironment interactions not revealed by diffusion MRI. In the current study, we observed a significant reduction of NAA T2 relaxation time in year 2 follow-up compared to baseline. Our previous study observed a significant NAA T2 relaxation time shortening in chronic SZ compared to healthy control but did not reach significance.[19] The NAA T2 relaxation time did not show significant difference between the patient and control groups at baseline and the first two years of follow-up in the current work. Our most recent cross-sectional study with a large sample size found that NAA T2 relaxation time of chronic psychosis was significantly lower compared to that of first episode psychosis, whereas

the NAA T2 of healthy controls did not vary with age.[24] Because NAA is located intracellularly and almost exclusively localized to neurons, the shortened NAA T2 relaxation time suggests intra-axonal abnormalities in psychosis, possibly due to increased interactions with intracellular macromolecules. This could be related to the intracellular macromolecule modifications such as cytoskeletal abnormalities.[45] Although the specific cause of the modification of NAA T2 relaxation time has not been discovered, our most recent study showed the widely reported NAA reduction in psychosis could be mostly contributed by T2 relaxation caused by cellular microenvironment alterations rather than true concentration reduction. And our current study further illustrates that this microenvironment change in neurons could happen earlier than the abnormalities of axon morphology implied by NAA ADC. The water T2 relaxation time showed a trend of increase without significance in the follow-up of psychosis, which confirm the results in our recent study.[24]

It has been recently reviewed that the extracellular space (ECS), which is the interconnected narrow gap between brain cells, occupies around 20% across different brain areas.[46, 47] The contributions of the different diffusion processes from the water in ECS, neurons and glia cells generate the unique diffusion behavior of water compared to NAA and choline. Decreased FA and increased diffusivity and T2 has been reported in patients with SZ[10, 11] and BD.[12] Our previous studies also observed increased water ADC[21] and T2[19] in chronic SZ patients compared to healthy controls. In the current study, we observed similar trends of water ADC and T2 in the patients compared to controls in year 2 follow-up but they did not reach significance (P = .146 and .147, respectively). It has been reviewed that the decreased FA was reported more widely and consistently in the chronic SZ studies than the FE SZ ones.[10] The current study shows a decrease of FA numerically but not significantly as the disease progresses, which is in line with the review. The nonsignificance of the water indices could be due to the small cohort.

Regarding the potential bias caused by subject movements, we compared the spectral qualities between the patient and the control groups. We ran the two-sample t-tests between two groups' SNR, linewidth and number of removed bad averages of $b0$ (P = .67, .15, .75, respectively) and the means of six gradient directions (P = .45, .15, .65, respectively). There was no significant difference between these measures, which suggests no evident spectral quality reduction in the patient group caused by the subject movements.

The present study must be considered in light of several limitations, including a relatively small sample, especially with a reduced subject number in year 2 follow-up. We used linear mixed models and not repeated Measures ANOVA to include all the data we have and give unbiased results in the presence of the missing values in year 2 follow-up. Additionally, patients were taking medication. The effect of antipsychotic medications on metabolite T2 relaxation times and ADC has not been studied. In the current study, we did not uncover a relationship between CPZ equivalents and metabolite T2 relaxation times or ADC, suggesting that the dose of antipsychotic medication did not have an effect on our measures. Supplementary table S2 compares the ADC values reported in literatures. A moderate b-value could lead to a higher estimate of ADC[35,48–53] as well as insufficient attenuations of the metabolites. The higher ADC values reported by the current study could also stem from the underestimated b-value, which was calibrated using the water ADC in a phantom and did not fully address the contributions from gradients from B_0 inhomogeneity or cross-terms with the slice-selection and spoiler gradients.[54] Higher b values with more accurate calculations and with bipolar diffusion gradients[55] will be considered for the future studies. Lastly, the mechanism of T2 relaxation alterations, as well as the relationship between the T2 relaxation time and diffusion remain unclear. Furthermore, there was contribution of diffusion to the T2 relaxation time we measured.[56] We performed the Pearson's R test between the patient group's NAA ADCs and T2 relaxation time of each time point and between different time points and found no significant correlation. This implies that although both T2 relaxation time and diffusion reflect the intracellular microenvironment, they may be governed by relatively independent aspects of this microenvironment.

In conclusion, the current work presents a longitudinal study of microstructural abnormalities in the WM of first episode psychosis and two yearly follow-up timepoints through the relaxation and diffusion of different metabolites and water. The findings confirm previously reported WM abnormalities in FE and chronic psychosis based on longitudinal observation of the same group of subjects. Furthermore, this study provides more detailed information on active neuroprogressive processes involving WM abnormalities including but not limited to glia and axons, bridging our understanding of disease evolution from FE to chronic disease. The changes in Cho vs. NAA over time, which reflect the differentiation of neuronal and glial abnormalities, are unique and they are potentially important for our understanding of disease mechanism. These findings have implications for the development of interventions aimed at targeting these processes while they are active and amenable to change.

Supplementary Material

Supplementary material is available at *Schizophrenia Bulletin*.

Funding

This work was supported by The National Institute of Mental Health (R21MH114020 (F.D.), P50MH115846 (D.O.) and R01MH114982 (F.D.).

Acknowledgment

The authors have declared that there are no conflicts of interest in relation to the subject of this study.

References

1. Stephan KE, Friston KJ, Frith CD. Dysconnection in schizophrenia: from abnormal synaptic plasticity to failures of self-monitoring. *Schizophr Bull.* 2009;35(3):509–527.
2. Paus T, Keshavan M, Giedd JN. Why do many psychiatric disorders emerge during adolescence? *Nat Rev Neurosci.* 2008;9(12):947–957.
3. Kubicki M, McCarley R, Westin CF, et al. A review of diffusion tensor imaging studies in schizophrenia. *J Psychiatr Res.* 2007;41(1–2):15–30.
4. Canu E, Agosta F, Filippi M. A selective review of structural connectivity abnormalities of schizophrenic patients at different stages of the disease. *Schizophr Res.* 2015;161(1):19–28.
5. Hatton SN, Lagopoulos J, Hermens DF, Hickie IB, Scott E, Bennett MR. White matter tractography in early psychosis: clinical and neurocognitive associations. *J Psychiatry Neurosci.* 2014;39(6):417–427.
6. Linke J, King AV, Poupon C, Hennerici MG, Gass A, Wessa M. Impaired anatomical connectivity and related executive functions: differentiating vulnerability and disease marker in bipolar disorder. *Biol Psychiatry.* 2013;74(12):908–916.
7. Benes FM, Majocha R, Bird ED, Marotta CA. Increased vertical axon numbers in cingulate cortex of schizophrenics. *Arch Gen Psychiatry.* 1987;44(11):1017–1021.
8. Akbarian S, Bunney WE Jr, Potkin SG, et al. Altered distribution of nicotinamide-adenine dinucleotide phosphate-diaphorase cells in frontal lobe of schizophrenics implies disturbances of cortical development. *Arch Gen Psychiatry.* 1993;50(3):169–177.
9. Selemon LD, Goldman-Rakic PS. The reduced neuropil hypothesis: a circuit based model of schizophrenia. *Biol Psychiatry.* 1999;45(1):17–25.
10. Pettersson-Yeo W, Allen P, Benetti S, McGuire P, Mechelli A. Dysconnectivity in schizophrenia: where are we now? *Neurosci Biobehav Rev.* 2011;35(5):1110–1124.
11. Kelly S, Jahanshad N, Zalesky A, et al. Widespread white matter microstructural differences in schizophrenia across 4322 individuals: results from the ENIGMA Schizophrenia DTI Working Group. *Mol Psychiatry.* 2018;23(5):1261–1269.
12. Nortje G, Stein DJ, Radua J, Mataix-Cols D, Horn N. Systematic review and voxel-based meta-analysis of diffusion tensor imaging studies in bipolar disorder. *J Affect Disord.* 2013;150(2):192–200.
13. Mori S, Zhang J. Principles of diffusion tensor imaging and its applications to basic neuroscience research. *Neuron.* 2006;51(5):527–539.
14. Palombo M, Shemesh N, Ronen I, Valette J. Insights into brain microstructure from in vivo DW-MRS. *Neuroimage.* 2018;182:97–116.
15. Branzoli F, Ercan E, Valabrègue R, et al. Differentiating between axonal damage and demyelination in healthy aging by combining diffusion-tensor imaging and diffusion-weighted spectroscopy in the human corpus callosum at 7 T. *Neurobiol Aging.* 2016;47:210–217.
16. Choi JK, Dedeoglu A, Jenkins BG. Application of MRS to mouse models of neurodegenerative illness. *NMR Biomed.* 2007;20(3):216–237.
17. Le Belle JE, Harris NG, Williams SR, Bhakoo KK. A comparison of cell and tissue extraction techniques using high-resolution 1H-NMR spectroscopy. *NMR Biomed.* 2002;15(1):37–44.
18. Ercan E, Magro-Checa C, Valabregue R, et al. Glial and axonal changes in systemic lupus erythematosus measured with diffusion of intracellular metabolites. *Brain.* 2016;139(Pt 5):1447–1457.
19. Du F, Cooper A, Cohen BM, Renshaw PF, Öngür D. Water and metabolite transverse T2 relaxation time abnormalities in the white matter in schizophrenia. *Schizophr Res.* 2012;137(1–3):241–245.
20. Ongür D, Prescot AP, Jensen JE, et al. T2 relaxation time abnormalities in bipolar disorder and schizophrenia. *Magn Reson Med.* 2010;63(1):1–8.
21. Du F, Cooper AJ, Thida T, Shinn AK, Cohen BM, Ongür D. Myelin and axon abnormalities in schizophrenia measured with magnetic resonance imaging techniques. *Biol Psychiatry.* 2013;74(6):451–457.
22. Lewandowski KE, Ongür D, Sperry SH, et al. Myelin vs axon abnormalities in white matter in bipolar disorder. *Neuropsychopharmacology.* 2015;40(5):1243–1249.
23. Lewandowski KE, Du F, Fan X, Chen X, Huynh P, Öngür D. Role of glia in prefrontal white matter abnormalities in first episode psychosis or mania detected by diffusion tensor spectroscopy. *Schizophr Res.* 2019;209:64–71.
24. Kuan E, Chen X, Du F, Ongur D. N-acetylaspartate concentration in psychotic disorders: T2-relaxation effects. *Schizophr Res.* 2021;232:42–44.
25. Whitehurst TS, Osugo M, Townsend L, et al. Proton magnetic resonance spectroscopy of N-acetyl aspartate in chronic schizophrenia, first episode of psychosis and high-risk of psychosis: a systematic review and meta-analysis. *Neurosci Biobehav Rev.* 2020;119:255–267.
26. Ota M, Wakabayashi C, Sato N, et al. Effect of l-theanine on glutamatergic function in patients with schizophrenia. *Acta Neuropsychiatrica* 2015;27(5):291–296.
27. Bustillo JR, Lauriello J, Rowland LM, et al. Effects of chronic haloperidol and clozapine treatments on frontal and caudate neurochemistry in schizophrenia. *Psychiatry Res.* 2001;107(3):135–149.
28. Aoyama N, Theberge J, Drost DJ, et al. Grey matter and social functioning correlates of glutamatergic metabolite loss in schizophrenia. *Br J Psychiatry.* 2011;198(6):448–456.
29. Galińska-Skok B, Szulc A, Małus A, et al. Proton magnetic resonance spectroscopy changes in a longitudinal schizophrenia study: a pilot study in eleven patients. *Neuropsychiatr Dis Treat*. 2019;15:839–847.
30. Kraguljac NV, Morgan CJ, Reid MA, et al. A longitudinal magnetic resonance spectroscopy study investigating effects of risperidone in the anterior cingulate cortex and hippocampus in schizophrenia. *Schizophr Res.* 2019;210:239–244.
31. Wang M, Barker PB, Cascella N, et al. Longitudinal changes in brain metabolites in healthy subjects and patients with first episode psychosis (FEP): a 7-Tesla MRS study. *bioRxiv* 2020. doi:10.1101/2020.08.25.267419.
32. Baldessarini RJ. *Chemotherapy in Psychiatry*; New York: Springer Press; 2013.
33. Tkác I, Starcuk Z, Choi IY, Gruetter R. In vivo 1H NMR spectroscopy of rat brain at 1 ms echo time. *Magn Reson Med.* 1999;41(4):649–656.
34. Simpson R, Devenyi GA, Jezzard P, Hennessy TJ, Near J. Advanced processing and simulation of MRS data using the FID appliance (FID-A)-An open source, MATLAB-based toolkit. *Magn Reson Med*. 2017;77(1):23–33.

35. Genovese G, Marjańska M, Auerbach EJ, et al. In vivo diffusion-weighted MRS using semi-LASER in the human brain at 3 T: methodological aspects and clinical feasibility. *NMR Biomed.* 2021;34(5):e4206.
36. Ronen I, Budde M, Ercan E, Annese J, Techawiboonwong A, Webb A. Microstructural organization of axons in the human corpus callosum quantified by diffusion-weighted magnetic resonance spectroscopy of N-acetylaspartate and post-mortem histology. *Brain Struct Funct.* 2014;219(5):1773–1785.
37. Lundell H, Ingo C, Dyrby TB, Ronen I. Cytosolic diffusivity and microscopic anisotropy of N-acetyl aspartate in human white matter with diffusion-weighted MRS at 7 T. *NMR Biomed.* 2021;34(5):e4304.
38. Jenkinson M, Beckmann CF, Behrens TE, Woolrich MW, Smith SM. FSL. *Neuroimage.* 2012;62(2):782–790.
39. Benjamini Y, Hochberg Y. Controlling the false discovery rate: a practical and powerful approach to multiple testing. *J Roy Stat Soc Ser B (Methodological)* 1995;57(1):289–300.
40. Lin A, Andronesi O, Bogner W, et al.; Experts' Working Group on Reporting Standards for MR Spectroscopy. Minimum reporting standards for in vivo magnetic resonance spectroscopy (MRSinMRS): experts' consensus recommendations. *NMR Biomed.* 2021;34(5):e4484.
41. Miller BJ, Buckley P, Seabolt W, Mellor A, Kirkpatrick B. Meta-analysis of cytokine alterations in schizophrenia: clinical status and antipsychotic effects. *Biol Psychiatry.* 2011;70(7):663–671.
42. Pasternak O, Westin CF, Bouix S, et al. Excessive extracellular volume reveals a neurodegenerative pattern in schizophrenia onset. *J Neurosci.* 2012;32(48):17365–17372.
43. Pasternak O, Sochen N, Gur Y, Intrator N, Assaf Y. Free water elimination and mapping from diffusion MRI. *Magn Reson Med.* 2009;62(3):717–730.
44. Pasternak O, Westin CF, Dahlben B, Bouix S, Kubicki M. The extent of diffusion MRI markers of neuroinflammation and white matter deterioration in chronic schizophrenia. *Schizophr Res.* 2015;161(1):113–118.
45. Beasley CL, Pennington K, Behan A, Wait R, Dunn MJ, Cotter D. Proteomic analysis of the anterior cingulate cortex in the major psychiatric disorders: evidence for disease-associated changes. *Proteomics.* 2006;6(11):3414–3425.
46. Soria FN, Miguelez C, Peñagarikano O, Tønnesen J. Current techniques for investigating the brain extracellular space. *Front Neurosci.* 2020;14:570750.
47. Hrabetova S, Cognet L, Rusakov DA, Nägerl UV. Unveiling the extracellular space of the brain: from super-resolved microstructure to in vivo function. *J Neurosci.* 2018;38(44):9355–9363.
48. Ellegood J, Hanstock CC, Beaulieu C. Considerations for measuring the fractional anisotropy of metabolites with diffusion tensor spectroscopy. *NMR Biomed.* 2011;24(3):270–280.
49. Ingo C, Brink W, Ercan E, Webb AG, Ronen I. Studying neurons and glia non-invasively via anomalous subdiffusion of intracellular metabolites. *Brain Struct Funct.* 2018;223(8):3841–3854.
50. Branzoli F, Ercan E, Webb A, Ronen I. The interaction between apparent diffusion coefficients and transverse relaxation rates of human brain metabolites and water studied by diffusion-weighted spectroscopy at 7 T. *NMR Biomed.* 2014;27(5):495–506.
51. Zheng DD, Liu ZH, Fang J, Wang XY, Zhang J. The effect of age and cerebral ischemia on diffusion-weighted proton MR spectroscopy of the human brain. *AJNR Am J Neuroradiol.* 2012;33(3):563–568.
52. Harada M, Uno M, Hong F, Hisaoka S, Nishitani H, Matsuda T. Diffusion-weighted in vivo localized proton MR spectroscopy of human cerebral ischemia and tumor. *NMR Biomed.* 2002;15(1):69–74.
53. Fotso K, Dager SR, Landow A, et al. Diffusion tensor spectroscopic imaging of the human brain in children and adults. *Magn Reson Med.* 2017;78(4):1246–1256.
54. Deelchand DK, Auerbach EJ, Marjańska M. Apparent diffusion coefficients of the five major metabolites measured in the human brain in vivo at 3T. *Magn Reson Med.* 2018;79(6):2896–2901.
55. Ronen I, Valette J. Diffusion-weighted magnetic resonance spectroscopy. *eMagRes.* 2015;4:733–750. doi:10.1002/9780470034590.emrstm1471
56. Michaeli S, Garwood M, Zhu XH, et al. Proton T2 relaxation study of water, N-acetylaspartate, and creatine in human brain using Hahn and Carr-Purcell spin echoes at 4T and 7T. *Magn Reson Med.* 2002;47(4):629–633.